High-resolution Cloud Analysis Information derived from Himawari-8 data

SUZUE Hiroshi*, IMAI Takahito** and MOURI Kouki*

Abstract

The Meteorological Satellite Center (MSC) of the Japan Meteorological Agency (JMA) has developed a product called High-resolution Cloud Analysis Information (HCAI) as the successor to Satellite Cloud Grid Information Data (SCGID). The product, which has been provided to JMA meteorological observatories and other users since 7 July 2015, is composed of five elements: cloud mask (including dust mask), snow ice mask, cloud type, cloud top height and quality control information. The spatial resolution of each element is 0.02° in both latitude and longitude, making it higher than that of SCGID (0.20° latitude, 0.25° longitude). Each element is calculated using observational data from Himawari-8 and the Fundamental Cloud Product (FCP).

This high resolution allows HCAI to report local cumulonimbus clouds that are not highlighted in SCGID. It also reports the cloud top surface clearly and supports a reduced incidence of stratus or fog being erroneously identified as stratocumulus.

1 Introduction

Satellite Cloud Grid Information Data (SCGID) (Tokuno, 2002) developed by the Meteorological Satellite Center (MSC) of the Japan Meteorological Agency (JMA) was first provided to JMA meteorological observatories to support operational weather forecasting and determination of weather conditions (e.g., sunny, cloudy, etc.) in 1999. Until 7 July 2015, it was produced using Multi-functional Transport Satellite (MTSAT) series data. It covered the area from 52ºN to the equator and from 114ºE to 180ºE, and had a spatial resolution of 0.20° in latitude and 0.25° in longitude. SCGID was composed of five elements: total cloud amount, upper cloud amount, convective cloud amount, cloud top height and cloud type (clear[1], cumulonimbus, cirrus[2], middle cloud, cumulus, stratocumulus, stratus/fog and dense cloud[3]).

Observational data from Himawari-8, which started operation on 7 July 2015, have a higher spatial resolution and more bands (Table 1) than the MTSAT series (Bessho et al., 2016). Against such a background, JMA/MSC developed a product called High-resolution Cloud Analysis Information (HCAI) to make optimal use of these data and launched it on 7 July 2015.

Before HCAI is produced, the Fundamental Cloud Product (FCP) (Imai and Yoshida, 2016; Mouri et al., 2016a,b) is produced from Himawari-8 data and Numerical Weather Prediction (NWP) data of JMA. FCP is a level-2 product created for each infrared band pixel of Himawari-8 data. It consists of cloud mask (including surface condition data), cloud type (opaque/semi-transparent/fractional, etc.), cloud phase (ice/water/mixed) and cloud top height (every 100 meters). HCAI is produced using Himawari-8 and FCP data.

---

[1] No cloud
[2] Semi-transparent upper cloud
[3] Opaque upper cloud

* System Engineering Division, Data Processing Department, Meteorological Satellite Center
** Office of Observation Systems Operation, Observation Department, Japan Meteorological Agency
(Received September 1, 2015, Accepted November 4, 2015)

Table 1 AHI specifications

Band Number	Central Wavelength [μm]	Spatial Resolution at sub-satellite point [km]
01	0.47	1
02	0.51	1
03	0.64	0.5
04	0.86	1
05	1.6	2
06	2.3	2
07	3.9	2
08	6.2	2
09	6.9	2
10	7.3	2
11	8.6	2
12	9.6	2
13	10.4	2
14	11.2	2
15	12.4	2
16	13.3	2

2 Product Specifications

2.1 Coverage and Spatial Resolution

HCAI covers the area from 60°N to 60°S and from 80°E to 160°W (Fig. 1).

The spatial resolution of each grid is 0.02° in both latitude and longitude, making a total of 6,001 grid boxes for each.

2.2 Data Utilized

The following data are used for HCAI:

- Brightness Temperature (BT) of bands 08 (6.2 μm), 10 (7.3 μm) and 13 (10.4 μm) of the Advanced Himawari Imager (AHI) on board Himawari-8
- FCP (cloud mask (including surface condition data), cloud type and cloud top height)

2.3 Calculation Meteorological Parameters

The product incorporates the following meteorological parameters:

- Cloud mask (including dust mask) (presence or absence of cloud/dust)
- Snow ice mask (presence or absence of snow/ice)
- Cloud type (clear (Clr), cumulonimbus (Cb), cirrus (CH), middle cloud (CM), cumulus (Cu), stratocumulus (Sc), stratus/fog (St/Fg) and dense cloud (Dense))
- Cloud top height (every 100 meters)
- Quality control information (effects of stray light, quality of cloud mask, etc.)

2.4 Sample Products

AHI imagery (Fig. 2 (a), (b)) and a sample of HCAI (Fig. 2 (c) – (f)) for 0200 UTC on 10 April 2015 are given below.

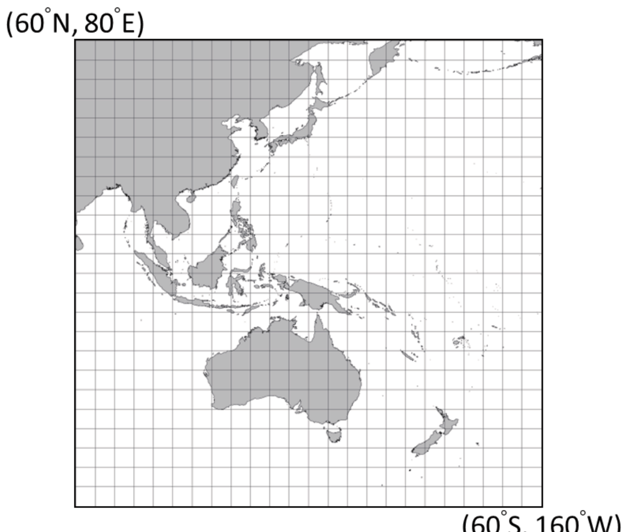

Fig. 1 Product coverage

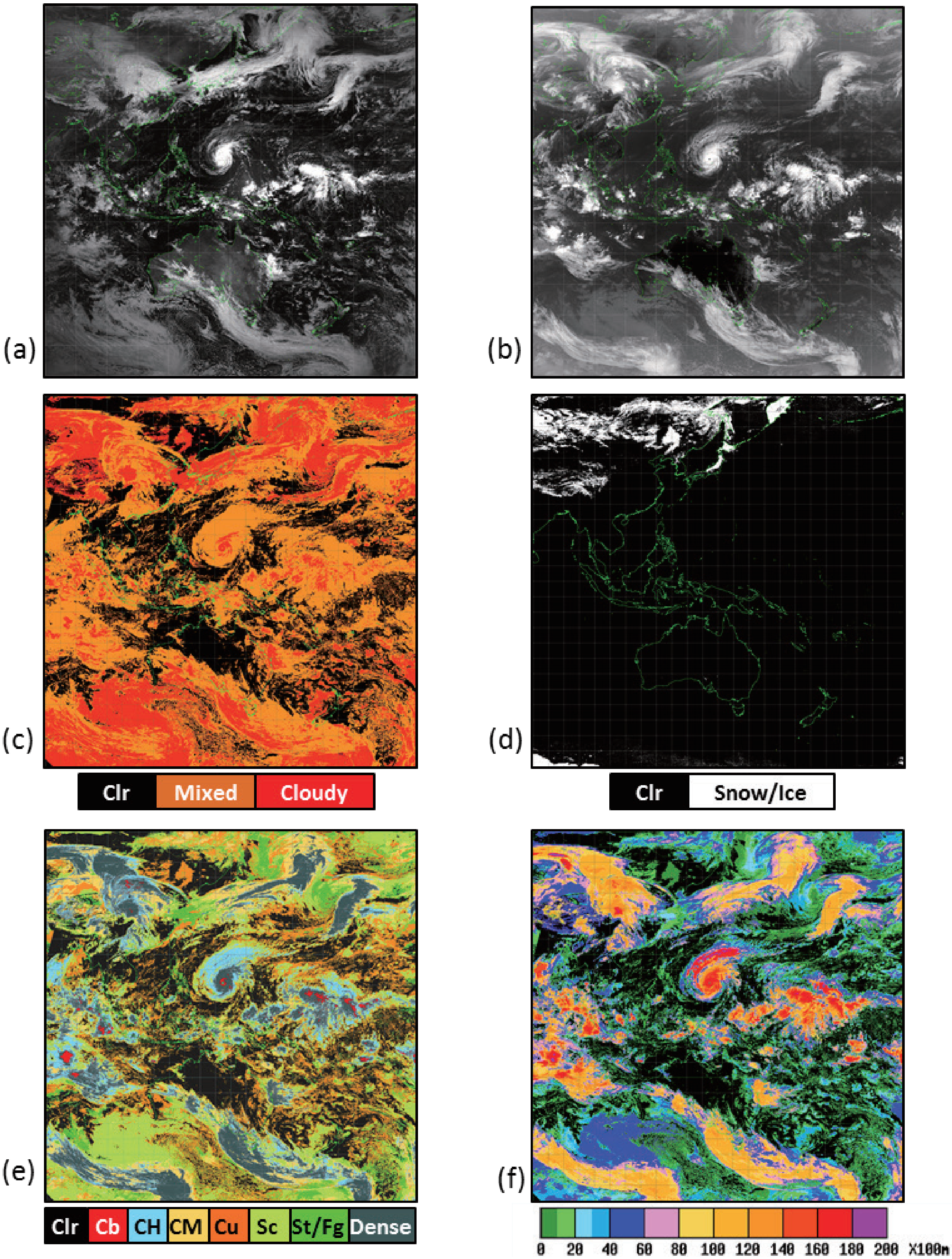

Fig. 2 (a) AHI imagery, band 03 (0.64 μm), (b) AHI imagery, band 13, (c) cloud mask, (d) snow ice mask, (e) cloud type and (f) cloud top height for 0200 UTC on 10 April 2015

3 HCAI Formulation Process

3.1 Calculation of Cloud Mask, Snow Ice Mask and Cloud Top Height

HCAI cloud mask, snow ice mask and cloud top height are derived from FCP via projection conversion. HCAI is produced from such conversion (for normalized geostationary projection) into equidistant cylindrical projection using the nearest-neighbor approach.

Quality flags for cloud mask and cloud top height include quality control information for HCAI as discussed in 3.3 below.

Snow ice mask is produced from FCP surface condition data. Snow ice is detected using the last four days of data and a snow depth product derived from data collected by microwave sensors on board low-earth-orbit (LEO) satellites. Accordingly, snow ice mask can provide data on snow ice below cloud levels.

3.2 Determination of Cloud Type

FCP cloud types include opaque, semi-transparent and fractional, while those in HCAI are expressed as cumulonimbus, dense cloud and the like. That is, FCP cloud types are based on optical or radiative properties, while those of HCAI are based on meteorological properties. Thus, the physical meanings of these cloud type expressions differ. Against such a background, and algorithm was developed to classify cloud types for HCAI. This element is produced using data such as FCP cloud type and AHI brightness temperature (bands 08, 10 and 13).

A flowchart of the classification algorithm for cloud type is shown below (Fig. 3), with BT(B10) and BT(B08) representing the brightness temperature of bands 10 and 08, respectively. maxBT(B13) and minBT(B13) are the maximum and minimum brightness temperatures of band 13 around the HCAI grid, respectively.

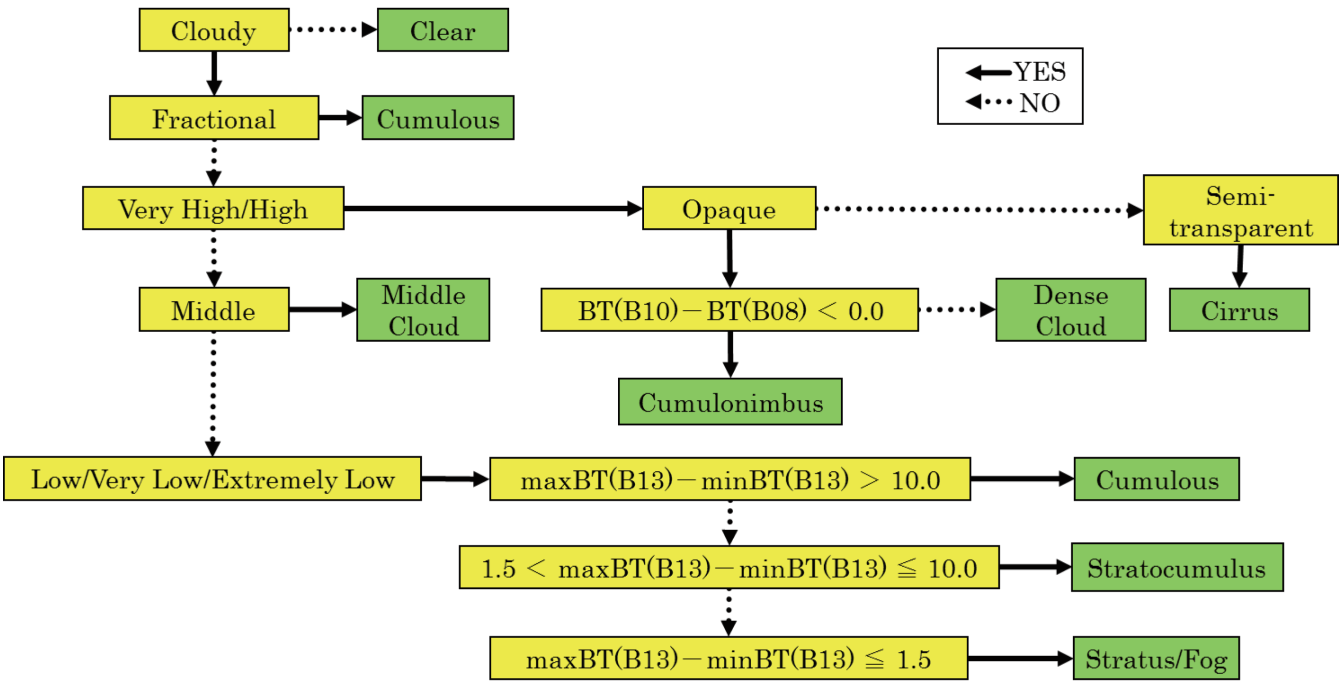

Fig. 3 Cloud type classification flowchart

3.3 Quality Control Information

Quality control information provides quality flags based on Himawari Standard Data (HSD) and FCP data.

HSD quality flags such as validity of quality, sun-related data degradation (e.g., sun avoidance, stray light), moon-related data degradation, solar calibration and solar eclipse are used for this information. FCP quality flags such as cloud mask, cloud type and cloud top height are also used.

Quality control information data are stored in each HCAI grid square in single bytes (eight bits). As shown in Table 2, eight elements are selected and allocated in order from the least significant bit. Quality is represented as zero (potentially high quality) or one (potentially low quality) for each bit.

Table 2 Details of quality control information

No.	Contents	0	1
1	Validity of Quality Flag	Valid	Invalid
2	Quality Loss due to the Effects of the Sun	No Possibility	Some Possibility
3	Quality Loss due to the Effects of the Moon	No Possibility	Some Possibility
4	Solar Calibration Operation	Not in Operation	In Operation
5	Solar Eclipse Operation	Not in Operation	In Operation
6	Quality of Cloud Mask	High Quality	Low Quality
7	Quality of Cloud Type	High Quality	Low Quality
8	Quality of Cloud Top Height	High Quality	Low Quality

4 Characteristics of Cloud Type Determination

4.1 Cumulonimbus

Figure 4 shows AHI imagery from band 03 (0.64 μm) (a), radar echo imagery (b), SCGID cloud type (c), and HCAI cloud type (d) for every hour from 0600 to 0800 UTC, when gusting winds caused damage in the Isesaki-shi area of Japan's Gunma Prefecture on 15 June 2015. The band 03 imagery and radar echo data facilitate understanding of how cumulonimbus developed.

Local cumulonimbus was not determined in SCGID due to its low spatial resolution (0.20° in latitude and 0.25° in longitude). Cumulonimbus was also not reported in SCGID even though convective cloud amount (cumulonimbus) is one of its elements (not shown). Meanwhile, local cumulonimbus was determined in Gunma, Fukushima and Miyagi prefectures in HCAI thanks to its high spatial resolution (0.02° in both latitude and longitude). This indicates that HCAI enabled detection of local cumulonimbus that was missed by SCGID.

4.2 Stratus/Fog

Figure 5 (a) provides imagery showing AHI differences between bands 07 (3.9 μm) and 13 including surface synoptic observations (SYNOP) when stratus or fog appeared over the eastern Sakhalin sea from the Sea of Japan to the northwest and in the Hidaka and Kushiro offings for 1200 UTC on 16 June 2015. Stratus or fog pushed into the interior of Hokkaido and China, and fog or mist was recorded in surface observation. The temperature in Kushiro was 13.1°C and the dew point temperature was 13.0°C, indicating significant atmospheric dampness. Figure 5 (b) shows an emagram of sonde observation at Kushiro for the same location as Fig. 5 (a). It indicates that an inversion layer formed from the ground toward the vicinity of 930 hPa, and that the lower layer was wet. Fog was likely to form with these conditions.

Figures 5 (c) and (d) show SCGID and HCAI cloud types, respectively, for the same location as Fig. 5 (a). In general, SCGID tends to suggest the presence of stratocumulus around stratus grid squares. This is seen in Fig. 5 (c), which indicates stratocumulus in the vicinity of Kushiro. Meanwhile, the smooth white region in Fig. 5 (a) is identified as stratus or fog in Fig. 5 (d). According to the latter, stratus or fog is present in the vicinity of Kushiro, which corresponds closely to the results of surface observation and the emagram.

It should be noted that it is difficult to determine from satellite observation whether the cloud base is grounded.

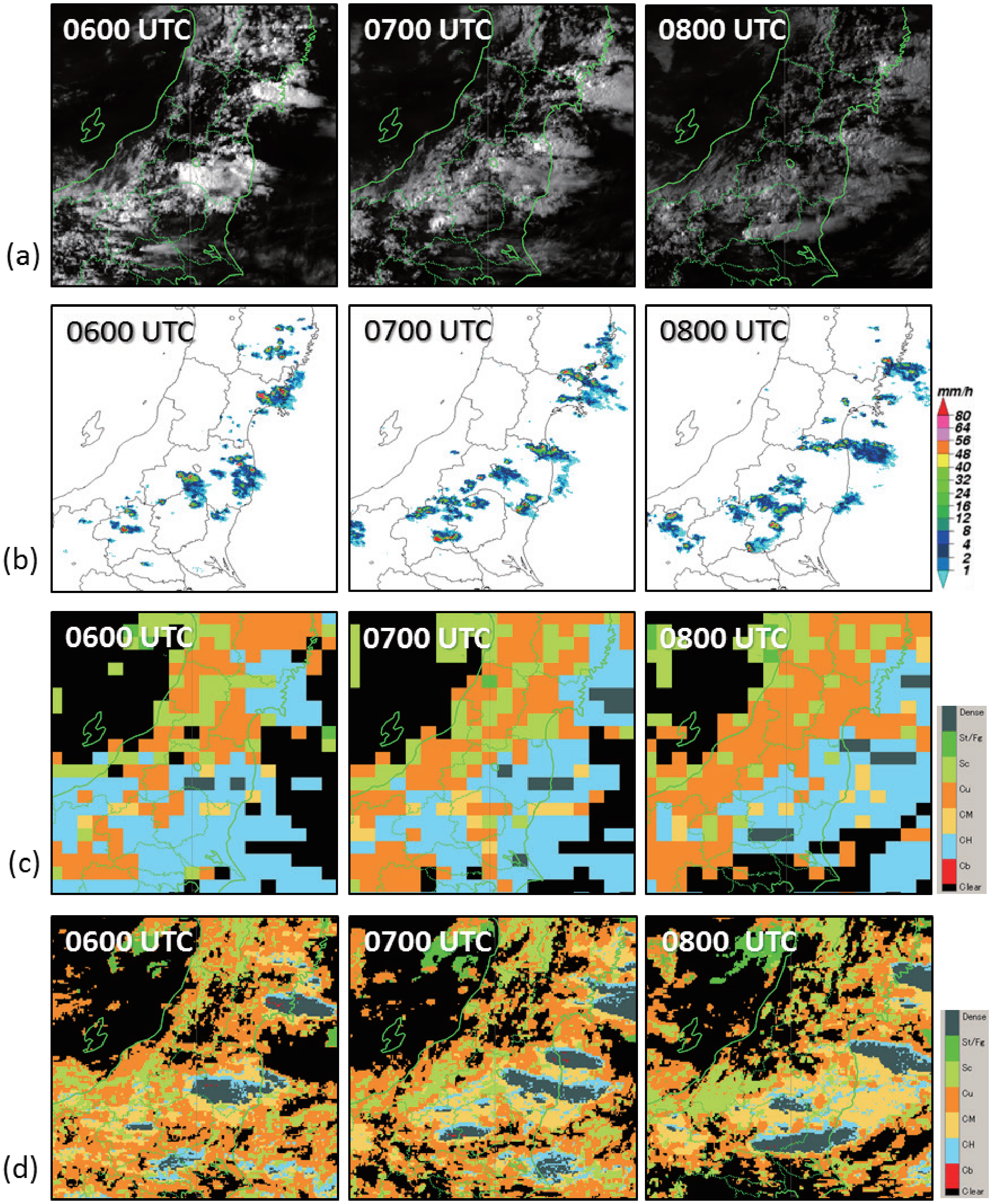

Fig. 4 (a) AHI imagery from band 03, (b) radar echo imagery, (c) SCGID cloud type and (d) HCAI cloud type for the period from 0600 to 0800 UTC on 15 June 2015

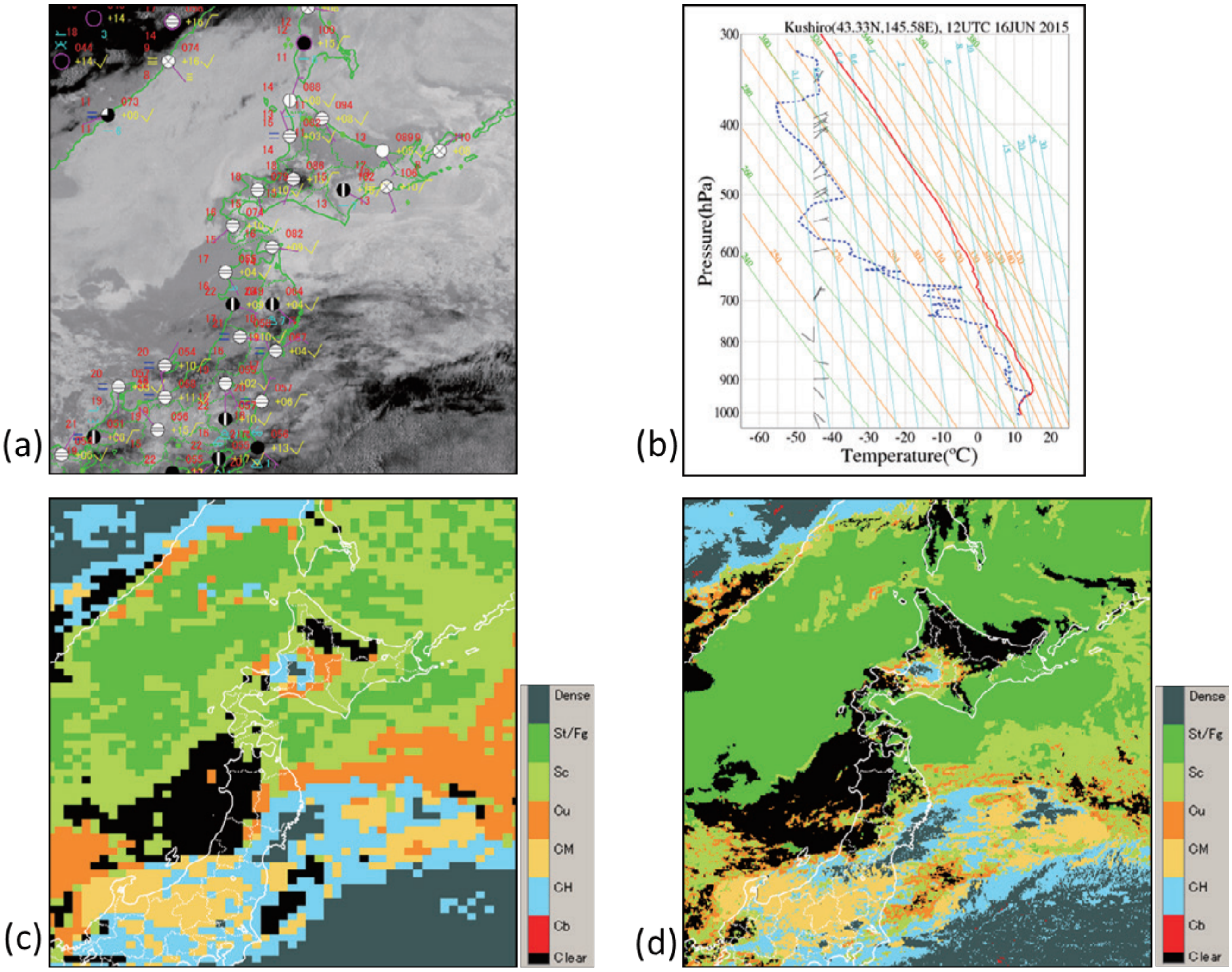

Fig. 5 (a) Imagery showing AHI differences between bands 07 and 13 including SYNOP, (b) emagram for Kushiro, (c) SCGID cloud type and (d) HCAI cloud type for 1200 UTC on 16 June 2015

The data are for 0000 UTC on 17 June 2015 after sunrise. Figures 6 (a) and (b) indicate that the vicinity of Kushiro was covered with low cloud with a smooth top. The surface observation data for Kushiro in Fig. 6 (a) indicate that the fog cleared. However, mist was still observed and produced poor visibility, and stratus was observed in the sky. The emagram in Fig. 6 (c) suggests that the inversion layer dissolved and wetness was low in the lower layer.

The SCGID cloud type data in Fig. 6 (d) indicate cumulus and stratocumulus near Kushiro. However, the HCAI data in Fig. 6 (e) show stratus or fog in the area, which corresponds closely with surface observation and the emagram for Kushiro.

5 Conclusions

MSC's HCAI product – the successor to the SCGID product – is based on observational data from Himawari-8 and FCP, and incorporates the five elements of cloud mask (including dust mask), snow ice mask, cloud type, cloud top height and quality control information. Its maximum coverage is from 60°N to 60°S and from 80°E to 160°W, and its spatial resolution is 0.02° in both latitude and longitude. It is capable of reporting local cumulonimbus and stratus/fog that are missed by SCGID, and is used for operational weather forecasting.

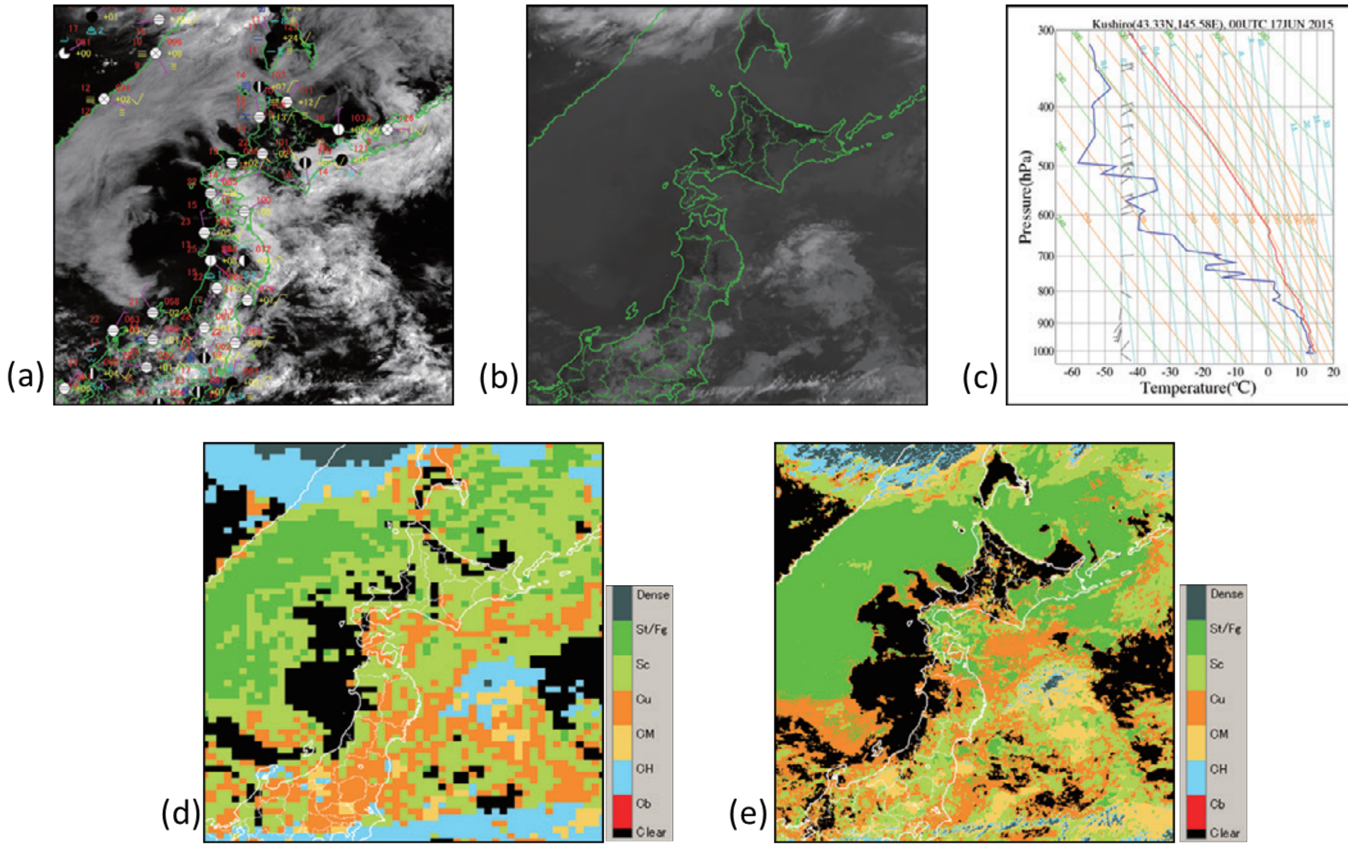

Fig. 6 (a) AHI imagery from band 03 including SYNOP, (b) AHI imagery for band 13, (c) emagram for Kushiro, (d) SCGID cloud type and (e) HCAI cloud type for 0000 UTC on 17 June 2015

References

Bessho, K., K. Date, M. Hayashi, A. Ikeda, T. Imai, H. Inoue, Y. Kumagai, T. Miyakawa, H. Murata, T. Ohno, A. Okuyama, R. Oyama, Y. Sasaki, Y. Shimazu, K. Shimoji, Y. Sumida, M. Suzuki, H. Taniguchi, H. Tsuchiyama, D. Uesawa, H. Yokota, and R. Yoshida, 2016: An introduction to Himawari-8/9 - Japan's new-generation geostationary meteorological satellites. *J. Meteor. Soc. Japan*, **94**, doi:10.2151/jmsj.2016-009.

Imai, T., and R. Yoshida, 2016: Algorithm theoretical basis for Himawari-8 Cloud Mask Product. *Meteorological Satellite Center Technical Note*, **61**, 1-17.

Mouri, K., T. Izumi, H. Suzue, and R. Yoshida, 2016a: Algorithm Theoretical Basis Document of Cloud Type/Phase Product. *Meteorological Satellite Center Technical Note*, **61**, 19-31.

Mouri, K., H. Suzue, R. Yoshida, and T. Izumi, 2016b: Algorithm Theoretical Basis Document of Cloud top height product. *Meteorological Satellite Center Technical Note*, **61**, 33-42.

Tokuno, M., 2002: Advanced Satellite Cloud Grid Information Data. *Meteorological Satellite Center Technical Note*, **40**, 1-24.

ひまわり 8 号による高分解能雲情報

鈴江　寛史*、今井　崇人**、毛利　浩樹*

要旨

気象衛星センターでは、雲量格子点情報の後継プロダクトである高分解能雲情報を開発し、2015 年 7 月 7 日から各地の気象官署等への配信を開始した。このプロダクトは雲の有無（ダストの有無を含む）、雪氷の有無、雲型、雲頂高度、品質情報の 5 つの要素から構成されている。各要素の空間分解能は 0.02°（緯度）×0.02°（経度）であり、これまでの 0.20°（緯度）×0.25°（経度）よりも高分解能となっている。各要素はひまわり 8 号観測データや基本雲プロダクトを利用して算出される。

高分解能になったことにより、これまで算出できなかったような小さい積乱雲を捉えることが可能となった。また、雲頂表面の凹凸を鮮明に捉えることが可能となり、層雲または霧域の周辺が層積雲と判別されることが少なくなった。

* 気象衛星センターデータ処理部システム管理課

** 気象庁観測部観測課観測システム運用室